Forkhead box A1 regulates prostate ductal morphogenesis and promotes epithelial cell maturation

Nan Gao[1,*], Kenichiro Ishii[2,*], Janni Mirosevich[2], Satoru Kuwajima[4], Stacey R. Oppenheimer[3,5], Richard L. Roberts[6], Ming Jiang[2], Xiuping Yu[2], Scott B. Shappell[6], Richard M. Caprioli[3,5], Markus Stoffel[4], Simon W. Hayward[2,3] and Robert J. Matusik[1,2,3,†]

[1]Department of Cell and Developmental Biology, Vanderbilt University, Nashville, TN 37232, USA
[2]Department of Urologic Surgery, Vanderbilt University, Nashville, TN 37232, USA
[3]Department of Cancer Biology and Vanderbilt-Ingram Cancer Center, Vanderbilt University, Nashville, TN 37232, USA
[4]Laboratory of Metabolic Diseases, The Rockefeller University, New York, NY 10021, USA
[5]Mass Spectrometry Research Center, Vanderbilt University, Nashville, TN 37232, USA
[6]Department of Pathology, Vanderbilt University, Nashville, TN 37232, USA

*These authors contributed equally to this work
†Author for correspondence (e-mail: robert.matusik@vanderbilt.edu)

Accepted 23 May 2005

Development 132, 3431-3443
Published by The Company of Biologists 2005
doi:10.1242/dev.01917

Summary

We have previously shown that a forkhead transcription factor Foxa1 interacts with androgen signaling and controls prostate differentiated response. Here, we show the mouse Foxa1 expression marks the entire embryonic urogenital sinus epithelium (UGE), contrasting with Shh and Foxa2, which are restricted to the basally located cells during prostate budding. The Foxa1-deficient mouse prostate shows a severely altered ductal pattern that resembles primitive epithelial cords surrounded by thick stromal layers. Characterization of these mutant cells indicates a population of basal-like cells similar to those found in the embryonic UGE, whereas no differentiated or mature luminal epithelial cells are found in Foxa1-deficient epithelium. These phenotypic changes are accompanied with molecular aberrations, including focal epithelial activation of Shh and elevated Foxa2 and Notch1 in the null epithelium. Perturbed epithelial-stromal interactions induced by Foxa1-deficient epithelium is evident, as demonstrated by the expansion of surrounding smooth muscle and elevated levels of stromal factors (Bmp4, Fgf7, Fgf10 and Gli). The prostatic homeobox protein Nkx3.1, a known proliferation inhibitor, was downregulated in Foxa1-deficient epithelial cells, while several prostate-specific androgen-regulated markers, including a novel Foxa1 target, are absent in the null prostate. These data indicate that Foxa1 plays a pivotal role in controlling prostate morphogenesis and cell differentiation.

Key words: Foxa1, Knockout, Prostate, Foxa2, Shh, Androgen, Mouse

Introduction

Gene inactivation studies in the mouse, combined with organ culture and tissue recombination, have highlighted the essential roles of androgenic signaling and epithelial-stromal interactions in directing prostate development. Key inductive and permissive factors must coordinately regulate early prostate morphogenesis and cell differentiation, but the regulatory mechanism by which various cellular signals synergize to induce the invariant prostate ductal pattern and promote gland maturation is still not fully understood (Marker et al., 2003; Abate-Shen and Shen, 2000).

Normal growth and differentiation of prostate epithelium is controlled through androgen-regulated paracrine signaling from the mesenchyme (Cunha et al., 1987), as the stromally located androgen receptor (AR) is essential for prostate epithelial differentiation (Donjacour and Cunha, 1993). In the absence of either androgens or stromal AR, the prostate does not develop (Bardin et al., 1973; Cunha et al., 1987). Conversely, reciprocal paracrine signals from the epithelium also patterns stromal cell differentiation (Cunha et al., 1996). Emerging evidence suggests that epithelial-mesenchymal interactions during prostate organogenesis involves several conserved families of molecules, including sonic hedgehog (Shh) (Podlasek et al., 1999; Lamm et al., 2002; Wang et al., 2003; Freestone et al., 2003; Berman et al., 2004), bone morphogenetic protein (Bmp) (Lamm et al., 2001), Fibroblast growth factors (Fgfs) (Thomson and Cunha, 1999; Donjacour et al., 2003), the Notch-Delta membrane molecule (Wang et al., 2004; Shou et al., 2001), and the Nkx3.1 homeobox protein (Bhatia-Gaur et al., 1999; Schneider et al., 2000; Tanaka et al., 2000).

Early prostate ductal budding and morphogenesis is accompanied by a transient elevation of multiple inductive pathway components (e.g. Shh, Bmp4, Fgf7, Fgf10 and Notch1), whose activities are dramatically downregulated at the conclusion of ductal morphogenesis (Podlasek et al., 1999; Lamm et al., 2001; Thomson et al., 1997; Thomson and Cunha, 1999; Wang et al., 2004). Among these factors, Shh is an epithelium-secreted ligand that plays a crucial role in prostate morphogenesis. Conflicting reports on Shh-elicited biologic

effects on the growth of the prostate ducts highlights the complex nature of this pathway. The differences between these studies could reflect a stage-dependent cellular response (Podlasek et al., 1999; Lamm et al., 2002; Freestone et al., 2003; Wang et al., 2003). In contrast to transient inductive signals, normal ductal growth also requires the sustained presence of negative modulators. For example, homeobox protein *Nkx3.1*-null mice show impaired prostate ductal growth and progressive epithelial hyperplasia (Bhatia-Gaur et al., 1999).

Previous biochemical analysis identified forkhead box a1 (Foxa1) as a key transcriptional component that interacts with AR on multiple prostatic enhancers and controls androgen-induced activation of both human and rodent prostate-specific genes (Gao et al., 2003). As forkhead transcription factors widely participate in the development of various organs (Carlsson and Mahlapuu, 2002), it was reasonable to expect that Foxa proteins may play an important role in prostate development, e.g. the specification/maturation of the prostate epithelial cell. Regulation of gut differentiation by Foxa homologues is a feature conserved in metazoa (Weigel and Jackle, 1990; Gaudet and Mango, 2002; Kalb et al., 1998; Horner et al., 1998) and in vertebrates, all three Foxa proteins (Foxa1, Foxa2 and Foxa3) are involved in the epithelial gut tube formation (Zaret, 1999; Zaret, 2002). The mouse prostate epithelium is derived from the hindgut endoderm and expresses Foxa1 throughout prostate development and maturation (Peterson et al., 1997; Kopachik et al., 1998; Gao et al., 2003), whereas it expresses Foxa2 only during prostate budding (Mirosevich et al., 2005). This suggests a potential role for these forkhead proteins in prostate development. Furthermore, the induction of multiple mammalian forkhead genes is dependent on the hedgehog signal in various tissues during embryogenesis (Chiang et al., 1996; Yamagishi et al., 2003; Furumoto et al., 1999; Mahlapuu et al., 2001). Thus, a better view of the precise distribution and regulation between these molecules in the embryonic urogenital sinus (UGS) is relevant to understanding the normal developmental process of the prostate. Here, we report the phenotypic and biochemical characterization of Foxa1-deficient mouse prostate using organ rescue and tissue recombination experiments. Our data demonstrate that epithelial Foxa1 plays an early role in prostate ductal morphogenesis, supporting a regulatory function that is essential for modulating inductive signals to control prostate cell growth and differentiation.

Materials and methods

Foxa1$^{-/-}$ mice, renal capsule rescue, and tissue recombination

Foxa1$^{-/-}$ mice on a C57/BL6 strain background were used (Shih et al., 1999). Entire prostatic rudiments from 64 male mice at P1 were grafted into renal capsules of adult male nude mice. PCR genotyping was performed and the distribution of *Foxa1*$^{+/+}$, *Foxa1*$^{+/-}$ and *Foxa1*$^{-/-}$ was 18, 33 and 13, respectively. Rescued organs were recovered from host mice at 2-15 weeks. Genotypes were re-confirmed on grafts by PCR or β-galactosidase staining.

E18 rat UGM was prepared for tissue recombination (Cunha and Donjacour, 1987). Bladder epithelial tissue fragments were separated from 89 P1 mice (24 *Foxa1*$^{+/+}$, 53 *Foxa1*$^{+/-}$ and 12 *Foxa1*$^{-/-}$), pooled by genotype and individually recombined with rUGM. Recombinants were grafted into adult male nude mice and harvested after 4 and 12 weeks. Grafting was performed in triplicate for each genotype at each time point.

In situ hybridization and RT-PCR

In situ hybridization for Foxa1 and Foxa2 was performed using digoxigenin-labeled gene-specific probes (Braissant and Wahli, 1998). For RT-PCR, total RNA was extracted with Qiagen^{TM} RNeasy extraction kit (Qiagen, Valencia). cDNAs were synthesized with 1.5 μg of total RNA by Superscript-II^{TM} reverse transcriptase (Invitrogen). PCR was performed using primer sets (see Table S1 in the supplementary material) to produce gene-specific fragments with optimal numbers of reaction cycle. Semi-quantitative analysis was performed by comparing the intensity of PCR product with normalization to an internal standard gene *Gapdh*.

β-Galactosidase staining

Fresh tissues were prefixed for 6 hours in 2% paraformaldehyde, 0.2% glutaraldehyde in PBS at 4°C, embedded in OCT. Frozen sections were immersed in the same solution for 10 minutes at 4°C, rinsed in water, and stained for β-galactosidase at 37°C for 1-6 hours.

Immunohistochemistry and immunofluorescence

Tissue preparation and staining procedures were as described (Mirosevich et al., 2005). Primary antibodies, at indicated dilutions, were AR (rabbit, 1:1000; Santa Cruz), Ck5 (rabbit, 1:500; Covance Research Products), Foxa2 (goat, 1:1000; Santa Cruz), Nkx3.1 (rabbit, 1:3000) (Kim et al., 2002), SMA (mouse, 1:1500; Sigma), γ-actin (mouse, B4, 1:10,000) (Lessard, 1988), Ck14 (mouse, 1:10), Ck8 (mouse, 1:10) (Wang et al., 2001), β-catenin (mouse, 1:200; BD Transduction Laboratories), p63 (rabbit, 1:200; Santa Cruz), Shh (rabbit, 1:200; Santa Cruz) (Thayer et al., 2003; Niemann et al., 2003; Krebs et al., 2003; Jaskoll et al., 2004) and Ptch1 (goat, 1:200; Santa Cruz) (Canamasas et al., 2003; Niemann et al., 2003; Di Marcotullio et al., 2004; Jaskoll et al., 2004; Sheng et al., 2004). Fluorescence-conjugated secondary antibodies (A11055, A21203, A21206, A21207) were purchased from Molecular Probes and diluted 1:200. DAPI staining was performed using Vectashield Mounting Medium (Vector, H-1200).

Electron microscopy

Tissues were fixed in 2% glutaraldehyde in 0.1M cacodylate buffer at 4°C overnight, dehydrated in alcohol and polymerized. Sections (70 nm) were cut and ultrastructural analysis was performed on Phillips CM-12 Transmission Electron Microscope equipped with AMT digital camera system.

Matrix assisted laser desorption ionization time-of-flight mass spectrometry

MALDI-TOF MS analysis was performed using a modified protocol (Chaurand et al., 2004). Using a cryostat, 10 μm prostate tissue sections were cut and mounted onto a conductive glass MALDI plate. Three or four sections were obtained per specimen and were stained with MALDI-compatible Cresyl Violet (Chaurand et al., 2004) to identify regions for profiling, Target areas were then spotted with 150 nl of saturated sinapinic acid as matrix prepared in acetonitrile/H_2O/TFA (50/50/0.1) by volume and allowed to dry. Each section was then analyzed by MALDI-TOF MS in the linear mode using an Applied Biosystems Voyager DE-STR mass spectrometer (Framingham, MA). Acquired spectra were baseline subtracted and normalized. Spectra from each prostate sample were then averaged before comparison.

Results

Distribution of Foxa1 and Foxa2 in mouse UGS

The embryonic UGS is a simple tubular structure containing a

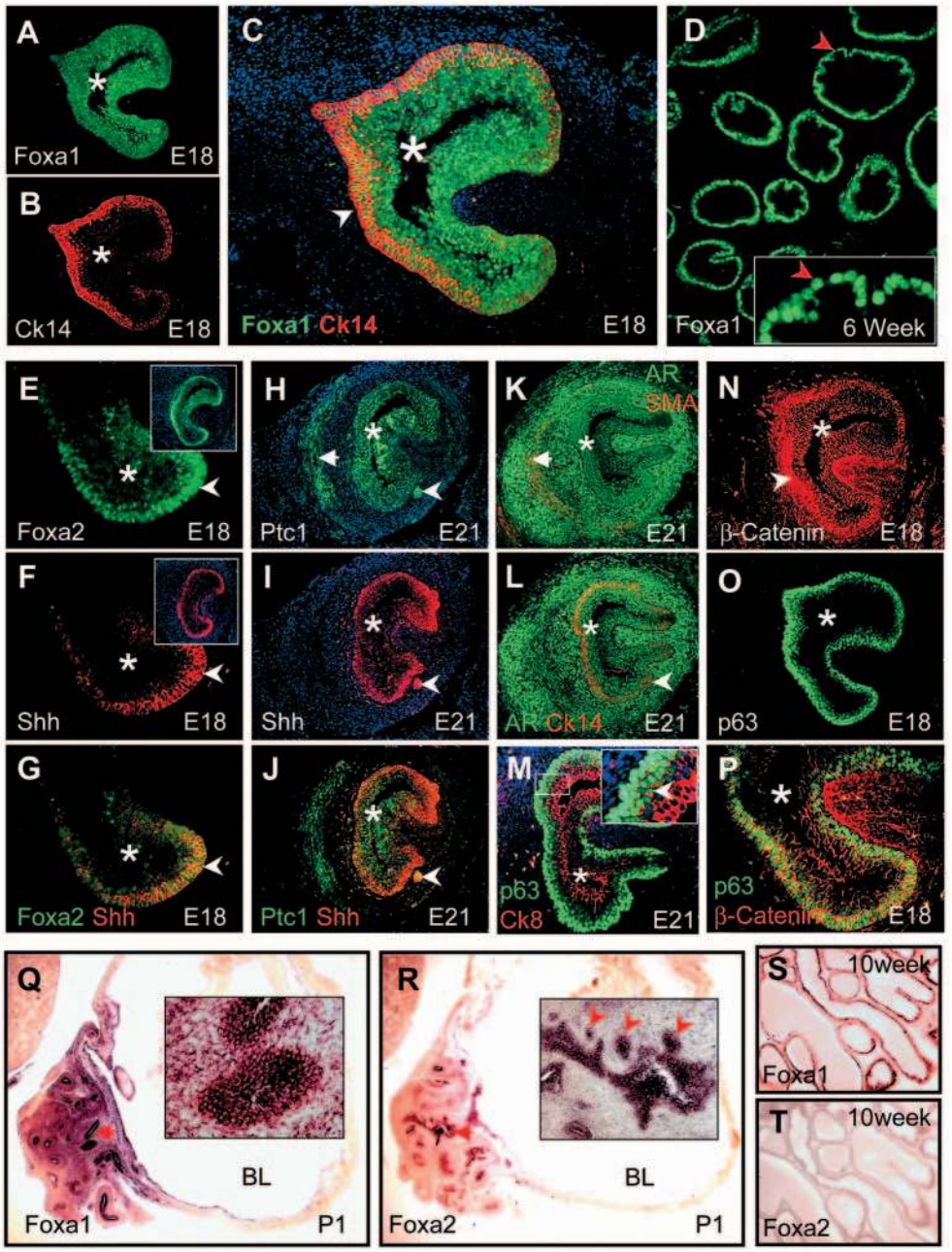

Fig. 1. Distribution of Foxa1 and Foxa2 in mouse UGS. (A) Foxa1 (green) is expressed in E18 mouse UGE (asterisk). (B) Ck14 staining (red) reveals peripheral basal epithelial layers. (C) Triple immunofluorescence merges from A and B, plus DAPI. (D) Nuclear Foxa1 staining (inset) is seen in 6-week-old mature prostate epithelium. (E) E18 UGE expresses Foxa2 (green nuclear staining) with strongest level in peripheral basal epithelium. Inset shows entire UGS counterstained with DAPI. (F) Same basal epithelial cells express Shh (red signal on cell-membrane). (G) Merges of E and F. (H) In E21 UGS, Ptch1 (green) is expressed in both UGE and mesenchymal cells (arrow). Arrowhead indicates Ptch1-expressing nascent prostatic buds. (I) Shh is co-expressed in E21 UGE and nascent epithelial buds (arrowhead). (J) Merges of H and I. (K) E21 UGS double stained for AR (green) and SMA (red). SMA-expressing cells are the same population expressing Ptch1 (arrow). (L) E21 UGS double-stained for AR (green) and Ck14 (red). (M) E21 UGS double-stained for Ck8 (red) and p63 (green). (N) β-Catenin (red) is expressed in both epithelium and surrounding mesenchyme in E18 UGS, with strongest signal detected in the peripheral epithelium (arrowhead). (O) E18 UGS stained for p63. (P) Magnified merges of N and O. (Q,R) In situ hybridization. Foxa1 and Foxa2 are expressed in P1 prostate rudiments (arrows, parasagittal sections). Insets show strongly stained epithelial buds (arrowheads in R). (S,T) Foxa1, but not Foxa2, is expressed in mature glands. BL, Bladder.

multilayered urogenital sinus epithelium (UGE) and a surrounding undifferentiated mesenchyme. Prostatic morphogenesis is initiated at mouse embryonic day 17-18 (E17-18), with the epithelium budding into the urogenital sinus mesenchyme (UGM) (Cunha et al., 1987). Foxa1 expression was detected in E18 UGS (Fig. 1A), with positive immunoreactivity observed in all UGE cells, including the peripheral basally located cells that were positive for basal cytokeratin 14 (Ck14) (Fig. 1B,C). Ck14-positive and Ck14-negative epithelial cells express Foxa1 at similar levels (Fig. 1C). Prostate sections from a 6-week-old mouse showed strong nuclear Foxa1 staining in the epithelium (Fig. 1D), indicating that Foxa1 expression was maintained in the adult epithelium.

By contrast, UGS Foxa2 immunoreactivity in E18 was highest in the basally located cells immediately adjacent to the surrounding UGM (Fig. 1E). Epithelial cells localized proximal to the UGS lumen (asterisk) were either unstained or weakly stained for Foxa2. Dual staining revealed that Shh was co-expressed with Foxa2 (Fig. 1F,G) in these basally located cells, which give rise to the nascent prostatic buds. This is consistent with the ability of Shh to induce Foxa2 expression (Sasaki et al., 1997).

Dual-staining for Shh and patched 1 (Ptch1), the transmembrane receptor for Shh, showed that Shh was continuously expressed in the E21 UGE with strongest level observed in the peripheral basally located cells and in the nascent prostatic epithelial buds (arrowhead in Fig. 1I), and Ptch1 was co-expressed in these cells (Fig. 1H,J), consistent with a reported detection of epithelial Ptch1 in neonatal prostate ductal tips (Pu et al., 2004). In addition to the UGE

compartment, Ptch1 was also detected in a population of mesenchymal cells close, but not immediately adjacent to, the Shh-producing UGE (arrow in Fig. 1H). Approximately ten-cell layers separate these stromal Ptch1-expressing cells and the epithelial cell source of Shh. This distance is within an effective range of hedgehog signaling (Ingham and McMahon, 2001). Serial sections revealed that these Ptch1-positive stromal cells expressed smooth muscle α-actin (SMA) (arrow in Fig. 1K), a mesenchymal target of Shh (Weaver et al., 2003). Detection of Ptch1 in both UGE and UGM suggested that Shh may act in both a juxtacrine and a paracrine fashion. Interestingly, a scattered Shh staining was detected in adjacent UGM surrounding the Shh-producing UGE. As this anti-Shh antibody is raised against the N-terminal epitope (amino acids 41-200) of Shh and is able to detect both the membrane-bound and the secreted Shh-N peptide; the scattered staining is most probably due to immunoreactivity with the diffused Shh-N peptides. This has not been reported previously in UGS (Freestone et al., 2003; Berman et al., 2004).

Expression of AR was detected in all cells of E21 UGS, including the basally located epithelium (Fig. 1L). However, the staining was stronger in UGM when compared with UGE. Staining for p63, a basal cell nuclear protein highlighted the peripheral basal-like cell population (Fig. 1O). Although both p63 and Ck14 are specific for basal cells, p63 has been reported to be expressed in almost all basal cells, whereas Ck14 is only expressed in a subpopulation (Signoretti et al., 2000; Hudson et al., 2001). In E21 UGS, some UGE co-expressed the basal cell marker p63 and the luminal keratin Ck8 (Fig. 1M), indicating their immature/undifferentiated status (Wang et al., 2001).

Staining was also performed to localize β-catenin, a downstream effector of the Wnt pathway, which can promote endodermal genes including Foxa1 and Foxa2 (Sinner et al., 2004). β-Catenin was specifically localized to the membrane of both UGE and the surrounding UGM cells (Fig. 1N), with the strongest expression seen in p63-expressing basally located cells (Fig. 1O-P).

In contrast to Foxa1, which continued to be expressed in the postnatal developing prostate (Fig. 1Q) and adult glands (Fig. 1S), Foxa2 mRNA was strongly but transiently expressed only during ductal morphogenesis (Fig. 1R), and its expression decreased to undetectable levels in mature glands (Fig. 1T). Thus, the downregulation of Foxa2 during postnatal prostate development was confirmed by in situ hybridization.

Foxa1 regulates normal prostate ductal morphogenesis

Foxa1 mutant mice were generated using a targeting vector which deletes the Foxa1 DNA-binding domain and creates an in-frame fusion with the *Escherichia coli lacZ* gene (Shih et al., 1999). *Foxa1*$^{-/-}$ mice die neonatally, thus we used two distinct strategies, renal capsule organ rescue (Wang et al., 2000) and tissue recombination (Cunha and Donjacour, 1987), to assess the impact of Foxa1-deficiency on prostate development.

Prostate rudiments (asterisks in Fig. 2A) and adjacent seminal vesicles were dissected from postnatal day 1 (P1) Foxa1 pups. *Foxa1*$^{-/-}$ male mice of P1 contained prostate rudiments (n=13) that were histologically identical to wild type, indicating a normal prostatic induction at this stage. Entire prostate rudiments (n=64) were rescued by renal capsule grafting into intact male athymic nude mice. Grafted prostates were recovered at various intervals between 2 and 15 weeks. Rescued prostates and seminal vesicles were compared after fine dissections. *Foxa1*$^{-/-}$ prostate tissues (asterisk in Fig. 2D) were consistently smaller and solid, whereas controls were enlarged and contained secretions (Fig. 2B,C). As the transgene *lacZ* was driven by Foxa1 promoter in the mutant allele, β-galactosidase staining revealed *lacZ* expression in rescued Foxa1$^{+/-}$ (Fig. 2F) and *Foxa1*$^{-/-}$ prostate epithelium that showed a pronounced epithelial cell disorganization (Fig. 2G).

Histological analysis of rescued prostates (between 2 and 15 weeks) showed that *Foxa1*$^{-/-}$ prostate developed many solid epithelial cell cords with cribriform patterns, and no normal-appearing lumen was observed (Fig. 2J,P,R; see Fig. S1A,C in the supplementary material). In 4-week-old renal-rescued wild-type control prostates (Fig. 2K,M,O; see Fig. S1B,F in the supplementary material), a normal lumen lined with monolayer of luminal epithelial cells was observed, reflecting normal prostate development, as previously reported (Kurita et al., 2004; Berman et al., 2004). Although in the rescue experiments it is difficult to precisely define each lobe, based upon careful microdissection (with attention on the anatomic location referring to adjacent seminal vesicles) and determination of gross morphology, we compared rescued tissues as closely as possible on a lobe basis. Identical Foxa1-deficient phenotype was consistently observed in distinct prostate lobes dissected from all *Foxa1*$^{-/-}$ prostates examined (n=13), suggesting that Foxa1 regulates prostate epithelial ductal pattern regardless of lobe identity. Tentatively identified lobes are listed as ventral prostates (VPs) in Fig. 2, and dorsolateral prostates (DLPs) in Fig. S1 in the supplementary material.

AR staining did not suggest a protein level change in Foxa1-deficient prostate epithelial cells (Fig. 2L-O). The same results were obtained when distinct lobes were dissected (see Fig. S1A-H in the supplementary material). Notably, when extending the rescue period up to 12-15 weeks, *Foxa1*$^{-/-}$ prostates continued to demonstrate the growth of epithelial cords with no obvious ductal canalization or luminal formation (see Fig. S1C,G in the supplementary material). To confirm this alteration in epithelial ductal patterning and to rule out the possibility of histological artifacts during section preparation, 1 μm frozen sections from 12-week-old rescued prostates were stained with Toluidine Blue to define the prostate ductal structure. As shown in Fig. 2P, *Foxa1*$^{-/-}$ prostate contained 'balls' of disorganized epithelial cells with impaired luminal structure (arrowhead), while the wild-type prostate showed highly organized luminal cells with a normal lumen (arrowhead in Fig. 2Q). Staining for E-cadherin, an adhesion molecule expressed specifically on epithelial cell membrane, demonstrated a total loss of cell polarity in Foxa1-deficient epithelial cells (Fig. 2R and inset). By contrast, wild-type luminal epithelial cells lined the lumen in a highly organized pattern (arrowhead in Fig. 2S), as indicated by focused E-cadherin staining at epithelial cell conjunctions (inset).

Using normal embryonic inductive UGM, we performed tissue recombination experiments with *Foxa1*$^{-/-}$ epithelium to determine if normal ductal patterning would be obtained. Neonatal *Foxa1*$^{+/+}$ or *Foxa1*$^{-/-}$ mouse bladder epithelium were recombined with wild-type E18 rat (r) UGM. Fig. 2H shows

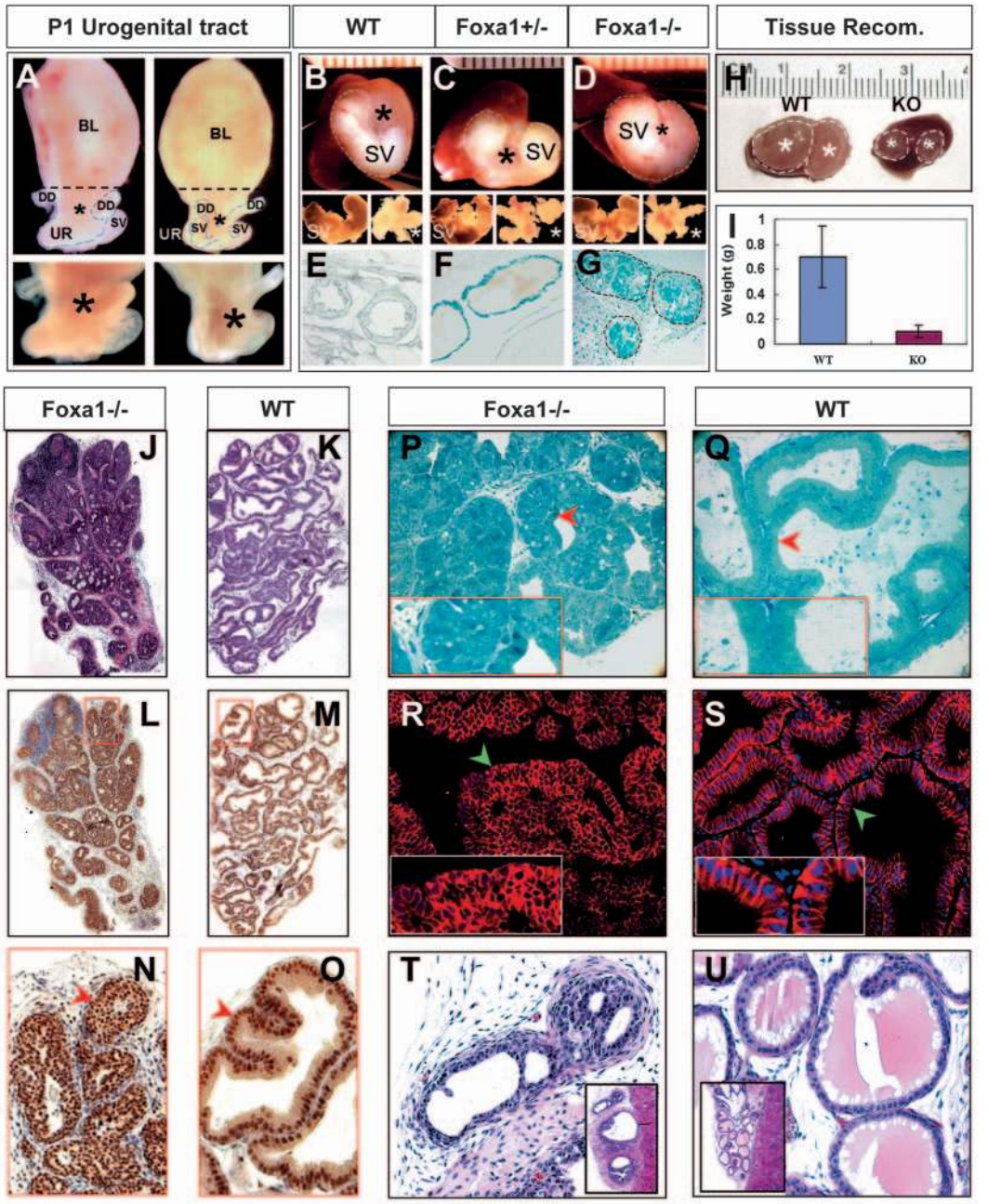

Fig. 2. Foxa1 regulates prostate ductal morphogenesis. (A) Upper panels: urogenital organs (lateral, left, and dorsal, right, views) dissected from P1 pups. The bladder was removed as indicated by broken lines. Lower panels: prostate rudiments (asterisks) and seminal vesicle (SV) were grafted as renal rescue tissue. (B-D) Upper panels: 8-week-old rescued tissues, with indicated genotypes, developed in the host renal capsules. SVs are circled with broken lines. Rescued *Foxa1*$^{-/-}$ prostate (asterisk in D) is smaller than controls upon comparison after fine dissection (lower panels). (E-G) β-Galactosidase staining on 8-week-old rescued prostates. (H) Twelve-week-old tissue recombinants derived from wild-type (left) or *Foxa1*$^{-/-}$ (right) epithelium that was recombined with E18 rUGM. (I) The *Foxa1*$^{-/-}$ recombinants have significantly lower weights than controls (n=3, P<0.01). (J-K) Hematoxylin and Eosin staining of 4-week-old rescued *Foxa1*$^{-/-}$ and *Foxa1*$^{+/+}$ VPs. (L,M) AR staining. (N,O) High magnification views of regions framed in L and M (arrowheads). (P,Q) Toluidine Blue staining on 1 μm thin section of 12-week-old rescued *Foxa1*$^{-/-}$ and wild-type VPs. (R,S) E-cadherin staining (red) on 12-week-old rescued *Foxa1*$^{-/-}$ and wild-type VPs. Foxa1-null epithelial cell polarity is disrupted (arrowheads). (T,U) Hematoxylin and Eosin staining of 12-week-old tissue recombinants from *Foxa1*$^{-/-}$ and control epithelium.

12-week-old grafted recombinants that were derived from wild-type (left) and Foxa1-deficient epithelium. The size and the wet weight (Fig. 2I) of null recombinants (n=15) were significantly smaller than control recombinants (n=15), even though the same number of wt rUGM cells were used (P<0.01). Histological analysis indicated that the embryonic rat UGM cells instructively elicited normal-appearing prostate glandular structure from wild-type bladder epithelium (Fig.

2U) as previously documented (Cunha et al., 1987); however, the same UGM cells failed to induce normal prostate architecture from *Foxa1*$^{-/-}$ epithelium (Fig. 2T), indicating a pivotal role for Foxa1 in determining the epithelial cell responsiveness to inductive mesenchymal signals.

Importantly, we detected a haploid insufficient phenotype in the dorsal prostates of intact Foxa1$^{+/-}$ mice (see Fig. S2 in the supplementary material). Although this phenotype was mild, the similar histological alteration indicated that the rescue and recombination experiments reflected the natural consequences of the loss of Foxa1.

Foxa1-deficient prostate shows an altered epithelial cell population and a modified stromal pattern

To define this phenotype, cell populations were examined from both rescue and recombinant prostates. In the normal mouse prostate, mature epithelium contains only a small proportion of basal cells (around 10%), whereas the luminal cells comprise the remaining epithelial cell type. Basal keratin Ck5 staining demonstrated a clear expansion of basal-like cells in *Foxa1*$^{-/-}$ prostates (4-week-old rescued prostate in Fig. 3A). Remarkably, in some Foxa1$^{-/-}$ epithelial ducts, these basal keratin-expressing cells became the predominant cell type, and their location was extended into the epithelial cords (Fig. 3B). Such a distribution of basal cells was not observed in any rescued wild-type prostates, rather basal cells are localized as a discontinuous layer between the luminal cells and the basement membrane (Fig. 3C). Basal keratin staining on tissue recombinants derived from wild-type and *Foxa1*$^{-/-}$ epithelium showed a similar expansion of basal-like cells in null recombinants (see Fig. S3A in the supplementary material).

Both the enrichment and the perturbed distribution of these basal keratin-expressing cells were reminiscent of a developmentally arrested prostate, similar to the basally located cells seen in the UGE prior to epithelial cell differentiation. Dual staining for p63 (a basal cell nuclear protein) and Ck8 (a luminal keratin) was used to further define the differentiation status of these *Foxa1*$^{-/-}$ cells. In mature prostate epithelium, these two markers segregate into distinct basal and luminal cell populations as solid epithelial cords differentiate (Wang et al., 2001; Hayward et al., 1996). Indeed this was recapitulated in rescued wild-type prostate where the expression of p63 (green) and Ck8 (red) was detected in segregated basal and luminal epithelial cells (Fig. 3E,G). By contrast, some Foxa1-deficient epithelial cells co-expressed p63 and Ck8 (Fig. 3D,F), strongly indicating that the null epithelium was arrested immaturely, as co-expression of p63 and Ck8 has only been observed transiently in normal embryonic UGE (Fig. 1M) or in early developing epithelium (Wang et al., 2001). In addition, dual staining for Ck14 and AR supported the observation that there was an increased number of Ck14-positive basal-like cells in Foxa1-deficient epithelial cords of different lobes (see Fig. S3C-H in the supplementary material).

Given that the loss of Foxa1 led to a failure of the prostate epithelium to mature, it seems likely that stromal patterning, which itself is dependent upon epithelial differentiation (Cunha et al., 1996), could also be abnormal. Staining for SMA revealed an expansion in smooth muscle layer that immediately surrounds the *Foxa1*$^{-/-}$ epithelial cords (Fig. 3H,I), suggesting mesenchymal hypercellularity. In the age-matched 4-week rescued wild-type prostate, only a thin layer of smooth muscle surrounded the ducts (Fig. 3J). Surprisingly, SMA staining on tissue recombinants revealed a more pronounced expansion of smooth muscle cells in recombinants that were derived

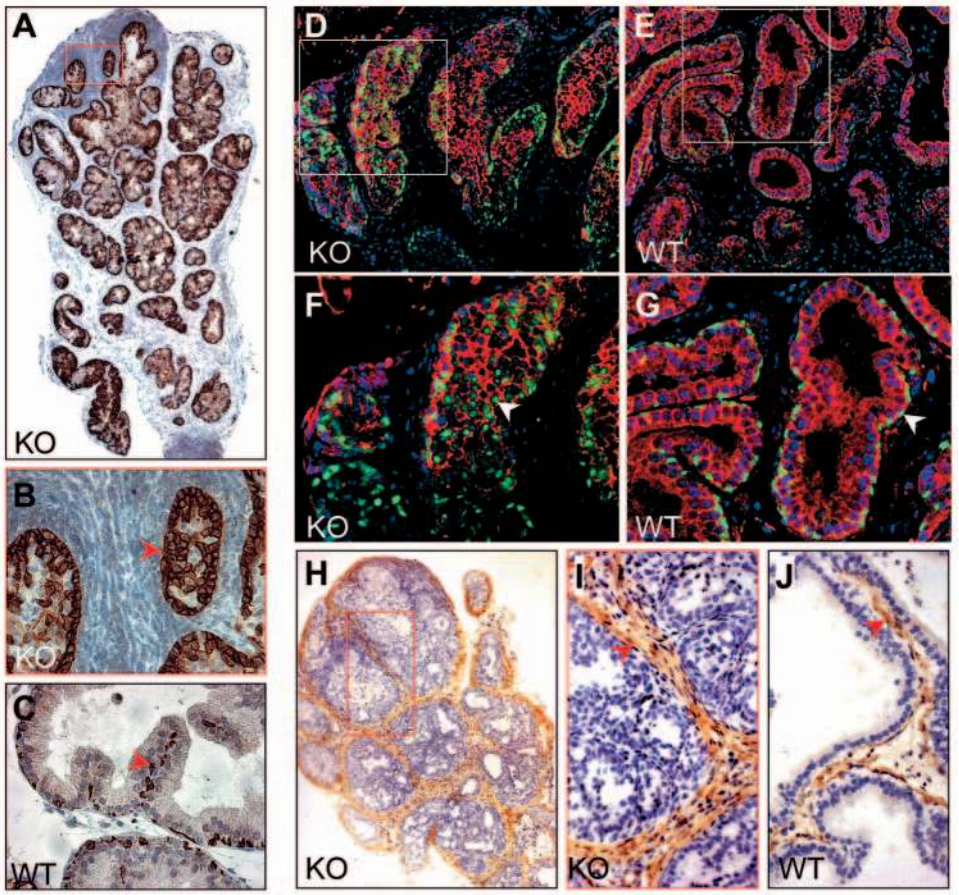

Fig. 3. Foxa1-deficient prostate has altered epithelial cell population and stromal pattern. (A) Ck5 staining on 4-week-old rescued *Foxa1*$^{-/-}$ VP. (B) Ck5-positive basal epithelial cells (arrow) expanded within the null epithelial cords. (C) Ck5 staining on rescued wild-type VP. (D,E) Dual-staining of p63 (green) and Ck8 (red) on 4-week-old rescued *Foxa1*$^{-/-}$ and *Foxa1*$^{+/+}$ DLPs. (F,G) Some *Foxa1*$^{-/-}$ cells co-expressed of both markers (arrowhead in F), while control cells expressed these markers separately (G). (H-J) SMA staining on 4-week-old rescued VPs. Expansion in smooth muscle layer (arrowheads) was seen in null prostate (H,I), but not in control (J).

from *Foxa1*$^{-/-}$ epithelium plus wild-type rUGM (see Fig. S3I in the supplementary material). The expression of smooth muscle γ-actin, a late marker for smooth muscle differentiation (Qian et al., 1996), was detected equally in wild-type and null recombinants (see Fig. S3K in the supplementary material), suggesting that although perturbed paracrine signaling from *Foxa1*$^{-/-}$ epithelium modified stromal pattern, smooth muscle cell differentiation was complete.

Foxa1$^{-/-}$ prostate is immature and devoid of secretory luminal cell

Semi-quantitative RT-PCR was performed on rescued prostates to examine the expression of several key inductive signaling molecules that correlate with early prostate morphogenesis (Podlasek et al., 1999; Thomson et al., 1997; Thomson and Cunha, 1999; Lamm et al., 2001; Wang et al., 2004) (Fig. 4). Gene expression profiles were compared after normalization to an internal standard gene *Gapdh*. Elevated mRNA levels of Shh, Gli2, Fgf7, Fgf10, Bmp4, β-catenin and Notch1 were detected in 4-week-old rescued *Foxa1*$^{-/-}$ prostates compared with controls. The continued presence of these molecules in the null prostate indicated that Foxa1 may be required for the maturation of the prostate. Interestingly, the expression of two other Gli proteins was either slightly increased (Gli1) or equally expressed (Gli3) in control and null tissues. However, the expression of Ihh, Bmp7 and Nkx3.1 were undetectable or decreased in the null. As the expression of Shh (Fig. 1F,I) and Notch1 (Wang et al., 2004) are associated with basally located epithelial cells in early developing prostate, elevation in both proteins supported an increased basal-like cell population in *Foxa1*$^{-/-}$ prostate.

Androgen stimulation induces the differentiation of immature prostate epithelium into luminal cells that produce prostate-specific secretory proteins (Kasper and Matusik, 2000). Transmission electron microscopy (EM) provides an unbiased way to determine secretory features of prostate epithelial cells at an ultrastructural level. EM analysis, on 12-week-old rescued wild-type prostate, showed tall columnar luminal epithelium (Fig. 5A), with enlarged Golgi complexes, and numerous dense secretory materials, the 'prostasomes' (Sahlen et al., 2002), within apical vesicles or at luminal surfaces (Fig. 5C). These ultrastructural features demonstrating secretory activities were completely absent in rescued *Foxa1*$^{-/-}$ epithelium (Fig. 5B,D).

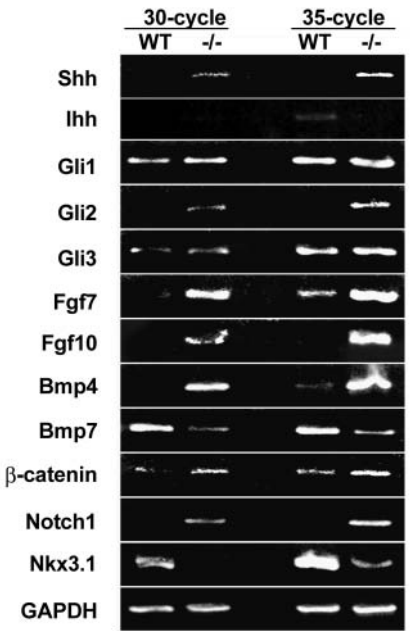

Fig. 4. Altered gene expression profiles in *Foxa1*$^{-/-}$ prostates. RT-PCR was performed using gene specific primers, on rescued *Foxa1*$^{+/+}$ and *Foxa1*$^{-/-}$ prostates, with *Gapdh* gene as an internal standard. Cycle numbers of amplification are indicated on the top.

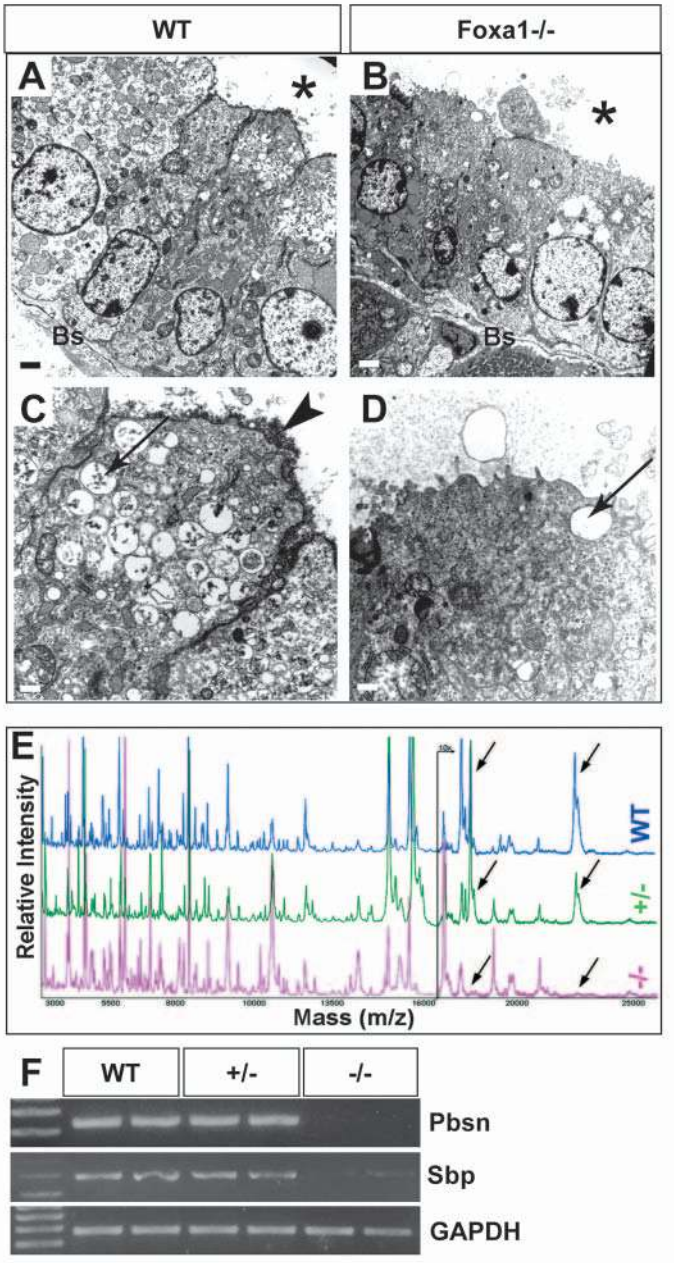

Fig. 5. No mature luminal cells in *Foxa1*$^{-/-}$ prostate. (A-D) EM analysis on 12-week-old rescued *Foxa1*$^{+/+}$ and *Foxa1*$^{-/-}$ VPs. Scale bars: 2 μm in A,B; 500 nm in C,D. Asterisks indicate the lumen. Wild-type cells (A,C) contain secretory materials seen in apical vesicles (arrow) and at luminal surface (arrowhead). Secretory material was absent in *Foxa1*$^{-/-}$ cells (B,D). (E) MALDI-MS protein profiles of m/z range 3000-16,000 obtained from 4-week-old rescued *Foxa1*$^{+/+}$, *Foxa1*$^{+/-}$ and *Foxa1*$^{-/-}$ prostates. Continuous profiles were zoomed in at m/z range 16,100-26,000. Arrows indicate peaks that were absent in *Foxa1*$^{-/-}$ but present in control prostates. (F) RT-PCR for Pbsn and Sbp. Bs, basement membrane.

Imaging mass spectrometry (IMS), which employs MALDI-TOF analysis of hundreds of 50 μm spots (approximately a five cell width) on frozen tissue sections to obtain a representative profile of low molecular weight proteins, has been used for profiling mouse prostate secretory proteins (Chaurand et al., 2001; Chaurand et al., 2004). IMS protein profiles obtained from 4-week-old rescued *Foxa1*$^{+/+}$, *Foxa1*$^{+/-}$ and *Foxa1*$^{-/-}$ prostates demonstrated that peaks at mass to charge ratios (m/z) of 18441 and 24781 (arrows) [consistent with the molecular weight of probasin (Pbsn) and prostatic spermine binding protein (Sbp) (Chang et al., 1987)] were detected in *Foxa1*$^{+/+}$ and *Foxa1*$^{+/-}$ prostates, but absent in *Foxa1*$^{-/-}$ prostates (Fig. 5E). Similar profiles were obtained from 12-week-old rescued prostates (data not shown).

RT-PCR was performed to validate the results obtained from IMS. Pbsn mRNA was completely undetectable in Foxa1-deficient prostates, while Sbp was dramatically decreased when compared with controls (Fig. 5F). Loss of Pbsn in *Foxa1*$^{-/-}$ prostates strongly supported our previous study that two forkhead response elements were essential for androgen-induced Pbsn expression (Gao et al., 2003). Interestingly, Sbp gene was identified in this study as a novel Foxa1 target. Examination of Sbp promoter revealed an organization of forkhead and androgen response elements that are similar to those seen in other androgen-regulated prostatic enhancers (see Fig. S4 in the supplementary material) (Gao et al., 2003). Whether these Foxa1-binding sites within the Sbp promoter are transcriptionally functional requires further investigation; however, the absence of secretory features and prostate differentiation markers in *Foxa1*$^{-/-}$ prostates do indicate a disruption in luminal epithelial cell maturation.

Perturbed epithelial-stromal interactions alter the null prostate ductal pattern

As phenotypic and molecular analysis on *Foxa1*$^{-/-}$ prostates indicated a perturbed epithelial-mesenchymal interaction, we examined potential pathways involving in signaling. Given that Shh regulates prostate ductal morphogenesis and deregulated hedgehog activity has been implicated in prostate diseases (Fan et al., 2004; Karhadkar et al., 2004; Sanchez et al., 2004), we examined Shh expression in rescued tissues. Strong and focused Shh expression was detected in rescued *Foxa1*$^{-/-}$ epithelial cell cords (Fig. 6A) and Shh-positive ductal epithelial buds were evident (Fig. 6B). As Ihh is absent the null prostate (Fig. 4), the pattern of Shh staining seen in *Foxa1*$^{-/-}$ prostate cannot be due to the antibody crossreactivity with Ihh. The same Shh-producing epithelium was positive for Ptch1 (Fig. 6C). However, no focused staining for Shh or Ptch1 was detected in rescued wild-type prostates (see Fig. S5A-C in the supplementary material and data not shown). By comparing the serial sections stained with SMA (Fig. 3H), we noted that Shh-expressing null epithelium (arrows in Fig. 6B) were surrounded by thick smooth muscle layers (see Fig. S5D,E in the supplementary material), in agreement with the finding that SMA is a mesenchymal target of Shh (Weaver et al., 2003). This suggests that the deregulated focal Shh activation in Foxa1-deficient epithelium may contribute to the altered epithelial-stromal interaction.

β-Catenin nuclear activation has been implicated in abnormal prostate epithelial cell growth (Bierie et al., 2003; Cheshire and Isaacs, 2003) and we observed an increase of β-catenin mRNA level in *Foxa1*$^{-/-}$ prostates (Fig. 4). However, we did not detect an increased nuclear level of β-catenin (red) in the p63-expressing basal-like cells (green) in *Foxa1*$^{-/-}$ epithelium (Fig. 6D). Instead, the signals are primarily localized to the cell membrane in both *Foxa1*$^{+/+}$ and *Foxa1*$^{-/-}$ epithelium (Fig. 6D,E). Nevertheless, the staining demonstrated a disrupted null epithelial cell polarity (Fig. 6D).

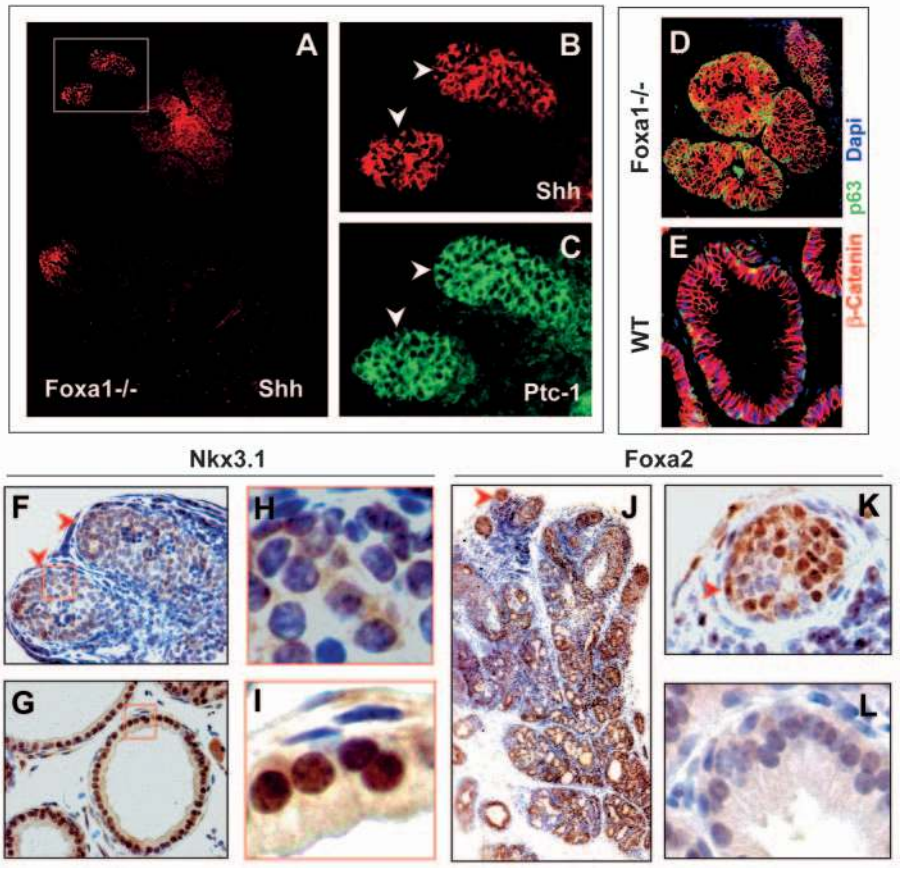

Fig. 6. Elevated Shh and Foxa2 but reduced Nkx3.1 expression in *Foxa1*$^{-/-}$ epithelium. (A) Shh expression in 4-week-old rescued *Foxa1*$^{-/-}$ VP epithelium, with strong and focused activity evident in the epithelial buds (B). (C) Ptch1 is detected in the same null epithelial buds. (D,E) Triple-immunofluorescence of β-catenin (red), p63 (green) and DAPI (blue) on rescued *Foxa1*$^{-/-}$ and *Foxa1*$^{+/+}$ prostates. (F-I) *Foxa1*$^{-/-}$ epithelium is negatively or faintly stained for nuclear Nkx3.1 (F,H). Arrowheads indicate the same epithelial buds illustrated in B. *Foxa1*$^{+/+}$ luminal epithelium show strong nuclear Nkx3.1 immunoreactivity (G,I). (J-L) Foxa2 is expressed in *Foxa1*$^{-/-}$ epithelium (J,K), but not in *Foxa1*$^{+/+}$ epithelium (L).

Nkx3.1 has been reported as the earliest known prostate-specific marker, and Nkx3.1-deficient mice show progressive epithelial cell hyperplasia (Bhatia-Gaur et al., 1999). RT-PCR showed a downregulation of Nkx3.1 mRNA in *Foxa1*$^{-/-}$ prostates (Fig. 4). Interestingly, *Foxa1*$^{-/-}$ epithelial buds that expressed Shh at a high level (Fig. 6B) showed weak or no nuclear staining for Nkx3.1 (Fig. 6F,H), while strong positive nuclear immunoreactivity was seen in rescued wild-type luminal epithelium (Fig. 6G,I).

Foxa2 is a target of Shh in the neural tube (Chiang et al., 1996; Hynes et al., 1997) and pharyngeal endoderm (Yamagishi et al., 2003); we have shown that Foxa2 expression overlaps with Shh in embryonic UGE (Fig. 1E-G), whereas Foxa2 is only transiently detected during prostate budding (Fig. 1R). Nuclear Foxa2 expression was retained in Foxa1$^{-/-}$ epithelium (Fig. 6J) even in prostates rescued for 15 weeks (see Fig. S5F in the supplementary material). These Foxa2-expressing cells tend to form tiny buds at ductal tips, suggesting that Foxa2 may closely correlate with epithelial cell growth and budding, a role consistent with its expression pattern during prostate budding (Fig. 1E). A similar correlation between elevated Foxa2 in Foxa1-null lung epithelium has been reported (Wan et al., 2005). Upon comparison of serial sections, nuclear Foxa2 staining was seen in Shh-expressing *Foxa1*$^{-/-}$ cells (Fig. 6K). Consistent with previous studies (Kopachik et al., 1998; Mirosevich et al., 2005), no detectable Foxa2 was seen in rescued *Foxa1*$^{+/+}$ prostates (Fig. 6L). Furthermore, this deregulated Foxa2 expression was confirmed in tissue recombinants derived from *Foxa1*$^{-/-}$ epithelium plus wild-type rUGM (see Fig. S5G in the supplementary material).

Discussion

In vertebrates, the endoderm gives rise to the epithelial lining of the respiratory and gastrointestinal tract, as well as to the lung, liver, thyroid, pancreas and hindgut derivatives, including the bladder and prostate (Wells and Melton, 1999; Cunha et al., 1987). In addition to common pathways that control endodermal development, the prostate has its own specific regulatory features, such as the androgenic signaling and the prostate-specific transcription factor Nkx3.1 (Abate-Shen and Shen, 2000). Cooperation of tissue-specific molecules with common transcription factors must be essential for the normal prostate ductal pattern and cell fate determination. In vitro studies revealed that an endoderm lineage regulator, Foxa1, modulates androgen-regulated differentiated response in cultured prostate epithelial cells (Gao et al., 2003). In this study, we reported a novel prostate phenotype resulting from Foxa1-deficiency, which is distinct from previously studied mutants with inactivated genes in AR (Tfm), Nkx3.1 or Shh. In addition to regulating prostate epithelial cell differentiation, Foxa1 also plays an early role in prostate ductal patterning.

The finding that Foxa1 participates in ductal morphogenesis is consistent with its early expression in embryonic UGE, during prostate budding, and ductal initiation. Although both Foxa1 and its closely related family member, Foxa2, are expressed in the early developing prostate epithelial buds, the distribution of Foxa2 is restricted to the basally located cell population, while Foxa1 is broadly expressed in almost all epithelium. Temporally, Foxa2 expression is downregulated to barely detectable levels shortly after birth, while Foxa1 is continuously expressed from early development to the maturation of the gland. This pattern is different from that observed in several other endodermal organs (e.g. lung and liver) where Foxa1 and Foxa2 co-express during adulthood (Zaret, 1999). In the prostate epithelium, the distinct spatial and temporal distribution of Foxa1 and Foxa2 suggest that these two transcription factors play different roles in prostate development. In Foxa1-deficient prostate epithelium, we observed sustained Foxa2 expression; however, continued Foxa2 expression does not rescue the Foxa1-deficient phenotype by compensating the loss of Foxa1, strongly arguing that the functions of these two proteins are divergent in the prostate. This result in the mouse prostate is different from the observation made in lung morphogenesis where Foxa1 and Foxa2 are functionally redundant (Wan et al., 2005). It is important to note that Foxa1 and Foxa2 are co-expressed in lung endoderm throughout adulthood, whereas only Foxa1 is expressed in the mature prostate epithelium.

The presence of primitive prostate structures in Foxa1-deficient mice indicates that this protein is not absolutely required for prostatic induction and the initial budding processes. The same observation has been made in Shh mutant mice whose prostatic buds can be induced upon renal capsule grafting or in vitro culture (Berman et al., 2004). However, different from Shh mutant prostates, whose ductal pattern is only minimally affected (Berman et al., 2004), the buds that are formed in Foxa1-deficient prostate do not follow the normal pattern of development and differentiation. Instead, structurally aberrant epithelial ducts demonstrate a hyperproliferative feature reminiscent of solid primitive epithelial cords that are surrounded by thick stromal layer. The abnormal ductal phenotype of Foxa1-deficient prostate is accompanied by a series of molecular aberrations, including maintained elevation in a number of early signaling molecules, most of which are involved in epithelial-mesenchymal interactions that induce and promote ductal morphogenesis. As Foxa1 is exclusively expressed in the epithelium, the altered expression of several stromal factors is probably due to a secondary effect caused by a perturbed epithelium-to-mesenchyme signaling induced by the Foxa1-null epithelium. Thus, persistent detection of early signaling molecules reflects a developmentally arrested feature of these Foxa1-deficient prostates.

We confirmed that the activation of Shh correlated with multiple reported targets (Ptch1, Gli, Foxa2 and Sma) in Foxa1-deficient prostate, where pathological features indicated cellular hyperproliferation in both epithelial and stromal cells. Taken together, our data suggest a correlation between Shh activity and the hyperproliferative features of the null prostate. Deregulated hedgehog pathway signaling has been identified in proliferative diseases such as prostate cancer (Fan et al., 2004; Karhadkar et al., 2004; Sanchez et al., 2004). It is conceivable that in Foxa1-deficient prostate, the deregulated hedgehog activity may be one of the causal factors that contribute to the abnormal ductal pattern. Our results agree with the fact that Shh is capable of inducing the growth of both epithelial and mesenchymal cells (Bellusci et al., 1997), and exert mitogenic effects on the development of various tissues (Lamm et al., 2002; Yu et al., 2002; Jaskoll et al., 2004; Thibert et al., 2003). Collectively, our data demonstrate that, in addition to a paracrine mechanism, Shh signaling may also act within the prostatic epithelium in a juxtacrine (or autocrine)

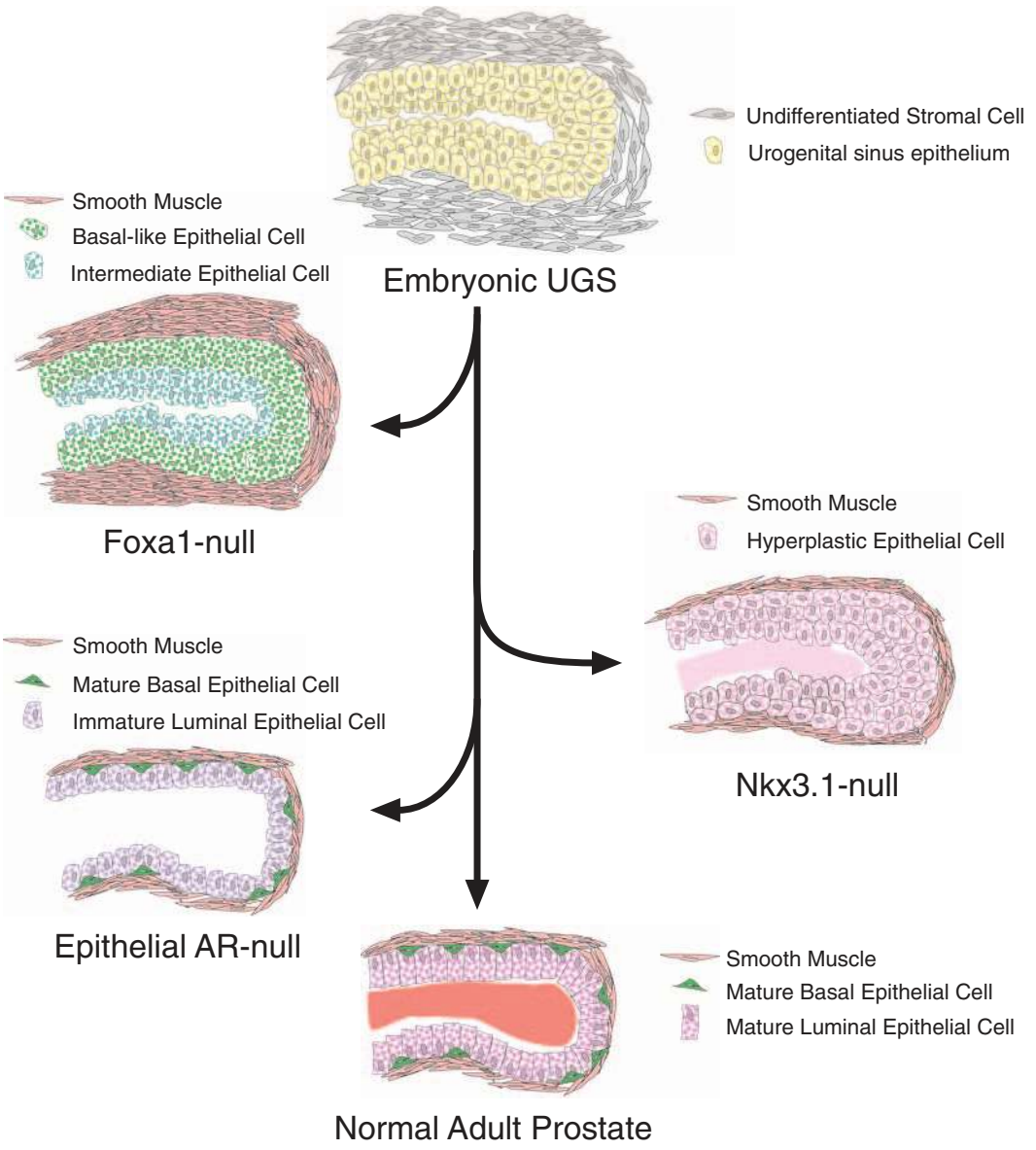

Fig. 7. Foxa1 regulates early ductal pattern formation and promotes epithelial cell maturation. The embryonic urogenital sinus is composed of undifferentiated epithelial and stromal cells. During early prostate morphogenesis, systemic androgens and elevated epithelial cell Foxa1 and Nkx3.1 proteins modulate cell growth and differentiation. The Foxa1-null prevents cytodifferentiation and results in a population of intermediate epithelial and basal-like cells that individually express markers representative of both cell types (i.e. Ck5, Ck8 and Ck14). The mesenchymal cells differentiate into an atypically thick layer of smooth muscle. Prostatic embryonic signaling pathways remain active as reflected by the elevation of Shh, Bmp, Fgf and Notch. Foxa2, which is normally expressed only in prostatic buds in the embryo, remains elevated while Nkx3.1 is downregulated. The Foxa1-null prostate produces limited secretory proteins. An *Nkx3.1*-null prostate shows an epithelial cell hyperplasia by four weeks of age with limited differentiation as reflected by dramatically reduced levels of secretory proteins. By 40 weeks of age, the Nkx3.1-null prostate contains both epithelial cells hyperplasia and prostatic intraepithelial neoplasia – a precursor lesion for prostate cancer. A prostate that has AR-null epithelium but retains AR in the stromal cells results in normal development of the ductal structural, including both epithelial and basal cells. However, full differentiation does not occur as secretory proteins are not expressed. The normal adult prostate exhibits functional cytodifferentiation with fully differentiated basal and luminal cells exhibiting a full profile of secretory activity.

manner. This provides an explanation for the hyperproliferation seen in *Foxa1*$^{-/-}$ epithelium. A similar model for Shh has been proposed in the mouse embryonic salivary gland epithelium (Jaskoll et al., 2004).

In prostate organ culture experiments, exogenous Shh treatment induced mesenchymal expansion in cultured postnatal rat ventral prostates (Freestone et al., 2003). This is consistent with our observation that the stromal layer is expanded in Foxa1-deficient prostates. However, abrogating hedgehog signaling by adding a chemical blocker, cyclopamine, induced an aberrant epithelial ductal pattern that resembles the Foxa1-mutant ductal structure (Freestone et al., 2003). One explanation is that these two studies used different experimental systems: Freestone et al. analyzed the effects of cyclopamine on the initial development of in vitro cultured prostate (P7) within a short period of time (Freestone et al., 2003), while renal-capsule rescue of *Foxa1*$^{-/-}$ prostate enabled us to determine the null prostate phenotype at various time points up to 15 weeks of age. We observed progressive growth of solid epithelial cords in the Foxa1 null with evident epithelial Shh expression, supporting a positive regulatory role of Shh on the ductal growth (Podlasek et al., 1999; Lamm et al., 2002). Alternatively, as already discussed (Wang et al., 2003), a global treatment of in vitro cultured prostate rudiments with chemical reagents may not precisely reflect the in vivo effects of spatially distributed signaling molecules.

We observed an overlapped expression of Shh and Foxa2 in the basally located epithelial cell population within the embryonic UGS. The Foxa2 promoter contains a Shh-responsive element (Sasaki et al., 1997), and Shh secreted from

the notochord induced Foxa2 expression in the floorplate of the neural tube; reciprocally Foxa2 maintained Shh expression in a positive feedback loop (Chiang et al., 1996; Hynes et al., 1997; Echelard et al., 1993; Sasaki et al., 1997). Detection of both Shh and Foxa2 in Foxa1-deficient prostate epithelium indicates that a reciprocal regulation between two proteins is actively present in these mutant prostates. This observation also suggests that Foxa1 could be a negative regulator that modulates the expression of Foxa2 or Shh in normal situation.

A novelty of Foxa1-deficent prostate phenotype is that the null epithelial cells have many features of the basally located epithelial cells that occur in embryonic UGS. These basal cells of the UGS are postulated to act as the transit/amplifying population in the prostate, and are widely believed to be capable of acting as luminal cell precursors (Abate-Shen and Shen, 2000). However, fully differentiated basal cells cannot be essential precursors to luminal cells as the p63-null prostates develop despite a lack of basal cells but they are required for ductal integrity (Kurita et al., 2004). In our study, no mature luminal epithelial cells were observed as defined by ultrastructural features or the expression of differentiation markers, suggesting that Foxa1 is essential for epithelial cell maturation. In addition, the prostate-specific transcription factor Nkx3.1 is also reduced in the Foxa1-deficient epithelium. Given the presence of forkhead binding sites in mouse and human Nkx3.1 gene enhancers (N.G., unpublished), one would speculate a potential regulatory mechanism may exist.

The relationship between various genetic changes and defects in prostatic development has been explored by a number of groups (summarized in Fig. 7). The normal prostate grows as a result of androgenically driven mesenchymal-epithelial cell interactions. In the normal prostate, this process results in the generation of solid epithelial cords that undergo ductal branching morphogenesis and cytodifferentiation giving rise to distinct basal and luminal cell populations. The luminal cells of the normal prostate express copious quantities of secretions (Cunha et al., 1987).

In the absence of epithelial AR (but in the presence of mesenchymal AR), prostatic development and differentiation can occur (Fig. 7). Tissue recombination experiments with AR-null epithelium results in prostatic tissue containing apparently normal basal and luminal cells. Glands have a well-defined lumen, but the luminal epithelial cells lack expression of prostatic secretory proteins (Cunha and Chung, 1981; Donjacour and Cunha, 1993). This demonstrates that epithelial AR is not required for prostatic development and cytodifferentiation but is required for the initiation and maintenance of secretory activity, the principle differentiated function of the luminal epithelial cells.

In the Nkx3.1-null mouse, the prostate develops a relatively normal ductal structure, albeit with reduced ductal branching and ductal tip number. Epithelial differentiation is somewhat disrupted with the formation of multilayered hyperplasia, notably in the anterior prostate, and in papillary tufts (Bhatia-Gaur et al., 1999). Epithelial cytodifferentiation, as reflected by secretory activity, is reduced (Fig. 7).

The Foxa1-deficient prostate is severely impeded in terms of ductal branching morphogenesis, even when compared with the Nkx3.1-null prostate. Ductal canalization and epithelial cytodifferentiation are profoundly inhibited. Differentiated secretory protein expression (e.g. Pbsn and Sbp) is absent even though there is a normal level of AR expression in the Foxa1-null epithelium. Previous work (Donjacour and Cunha, 1993) and our study have provided clear evidence that both AR and Foxa1 regulate prostate development, but Foxa1 plays an early role in promoting glandular morphogenesis and cytodifferentiation.

The most severe prostatic phenotype (a total failure to develop) can be elicited by loss of either stromal or total AR (for example in Tfm mice or in AIS humans) (Cunha et al., 1987). This demonstrates that stromal and epithelial AR functions are separate and distinct. Notably, Foxa1 probably functions at two levels acting both to control glandular morphogenesis and cytodifferentiation (present study) and secretory function (Gao et al., 2003).

Taken together, our study demonstrates that Foxa1 plays a pivotal role in prostate ductal morphogenesis and implies that this protein may crucially involve in modulating the balance of inductive and negative regulators to control prostate cell growth, differentiation and patterning.

We thank Dr Guangyu Gu for experimental advice, Manik Paul for technical assistance, Dr E. Birgitte Lane for providing the CK8 and CK14 antibodies, Dr James L. Lessard for γ-actin antibody, and Dr Cory Abate-Shen for Nkx3.1 antibody. This work was supported by NIH/NIDDK Grants R01-DK55748 and NIA R01-AG23490, and the Frances Williams Preston Laboratories of the T. J. Martell Foundation to R.J.M.; by NIH/NCI U01-CA96403 to S.W.H.; by NIH/NIGMS R01-GM58008 and NCI/NIDA R33-CA86243 to R.M.C.; by NIH/NIDDK R01-DK55033-07 to M.S.; by the Toxicology Training Grant T32ES07028-29 to S.R.O.; and by a Department of Defense Post doctoral Training Award W81XWH-04-1-0050 to J.M.

Supplementary material

Supplementary material for this article is available at
http://dev.biologists.org/cgi/content/full/132/15/3431/DC1

References

Abate-Shen, C. and Shen, M. M. (2000). Molecular genetics of prostate cancer. *Genes Dev*. **14**, 2410-2434.

Bardin, C. W., Bullock, L. P., Sherins, R. J., Mowszowicz, I. and Blackburn, W. R. (1973). Androgen metabolism and mechanism of action in male pseudohermaphroditism: a study of testicular feminization. *Recent Prog. Horm. Res.* **29**, 65-109.

Bellusci, S., Furuta, Y., Rush, M. G., Henderson, R., Winnier, G. and Hogan, B. L. (1997). Involvement of Sonic hedgehog (Shh) in mouse embryonic lung growth and morphogenesis. *Development* **124**, 53-63.

Berman, D. M., Desai, N., Wang, X., Karhadkar, S. S., Reynon, M., Abate-Shen, C., Beachy, P. A. and Shen, M. M. (2004). Roles for Hedgehog signaling in androgen production and prostate ductal morphogenesis. *Dev. Biol.* **267**, 387-398.

Bhatia-Gaur, R., Donjacour, A. A., Sciavolino, P. J., Kim, M., Desai, N., Young, P., Norton, C. R., Gridley, T., Cardiff, R. D., Cunha, G. R. et al. (1999). Roles for Nkx3.1 in prostate development and cancer. *Genes Dev.* **13**, 966-977.

Bierie, B., Nozawa, M., Renou, J. P., Shillingford, J. M., Morgan, F., Oka, T., Taketo, M. M., Cardiff, R. D., Miyoshi, K., Wagner, K. U. et al. (2003). Activation of beta-catenin in prostate epithelium induces hyperplasias and squamous transdifferentiation. *Oncogene* **22**, 3875-3887.

Braissant, O. and Wahli, W. (1998). Differential expression of peroxisome proliferator-activated receptor-alpha, -beta, and -gamma during rat embryonic development. *Endocrinology* **139**, 2748-2754.

Canamasas, I., Debes, A., Natali, P. G. and Kurzik-Dumke, U. (2003). Understanding human cancer using Drosophila: Tid47, a cytosolic product of the DnaJ-like tumor suppressor gene l2Tid, is a novel molecular partner of patched related to skin cancer. *J. Biol. Chem.* **278**, 30952-30960.

Carlsson, P. and Mahlapuu, M. (2002). Forkhead transcription factors: key players in development and metabolism. *Dev. Biol.* **250**, 1-23.

Chang, C. S., Saltzman, A. G., Hiipakka, R. A., Huang, I. Y. and Liao, S. S. (1987). Prostatic spermine-binding protein. Cloning and nucleotide sequence of cDNA, amino acid sequence, and androgenic control of mRNA level. *J. Biol. Chem.* **262**, 2826-2831.

Chaurand, P., DaGue, B. B., Ma, S., Kasper, S. and Caprioli, R. M. (2001). Strain-based Squence Variations and Structure Analysis of Murine Prostate Specific Spermine Binding Protein Using Mass Spectrometry. *Biochemistry* **40**, 9725-9733.

Chaurand, P., Schwartz, S. A., Billheimer, D., Xu, B. J., Crecelius, A. and Caprioli, R. M. (2004). Integrating histology and imaging mass spectrometry. *Anal. Chem.* **76**, 1145-1155.

Cheshire, D. R. and Isaacs, W. B. (2003). Beta-catenin signaling in prostate cancer: an early perspective. *Endocr. Relat. Cancer* **10**, 537-560.

Chiang, C., Litingtung, Y., Lee, E., Young, K. E., Corden, J. L., Westphal, H. and Beachy, P. A. (1996). Cyclopia and defective axial patterning in mice lacking Sonic hedgehog gene function. *Nature* **383**, 407-413.

Cunha, G. R. and Chung, L. W. (1981). Stromal-epithelial interactions–I. Induction of prostatic phenotype in urothelium of testicular feminized (Tfm/y) mice. *J. Steroid Biochem.* **14**, 1317-1324.

Cunha, G. R. and Donjacour, A. (1987). Mesenchymal-epithelial interactions: technical considerations. *Prog. Clin. Biol. Res.* **239**, 273-282.

Cunha, G. R., Donjacour, A. A., Cooke, P. S., Mee, S., Bigsby, R. M., Higgins, S. J. and Sugimura, Y. (1987). The endocrinology and developmental biology of the prostate. *Endocr. Rev.* **8**, 338-362.

Cunha, G. R., Hayward, S. W., Dahiya, R. and Foster, B. A. (1996). Smooth muscle-epithelial interactions in normal and neoplastic prostatic development. *Acta Anat. (Basel)* **155**, 63-72.

Di Marcotullio, L., Ferretti, E., De Smaele, E., Argenti, B., Mincione, C., Zazzeroni, F., Gallo, R., Masuelli, L., Napolitano, M., Maroder, M. et al. (2004). REN(KCTD11) is a suppressor of Hedgehog signaling and is deleted in human medulloblastoma. *Proc. Natl. Acad. Sci. USA* **101**, 10833-10838.

Donjacour, A. A. and Cunha, G. R. (1993). Assessment of prostatic protein secretion in tissue recombinants made of urogenital sinus mesenchyme and urothelium from normal or androgen-insensitive mice. *Endocrinology* **132**, 2342-2350.

Donjacour, A. A., Thomson, A. A. and Cunha, G. R. (2003). FGF-10 plays an essential role in the growth of the fetal prostate. *Dev. Biol.* **261**, 39-54.

Echelard, Y., Epstein, D. J., St Jacques, B., Shen, L., Mohler, J., McMahon, J. A. and McMahon, A. P. (1993). Sonic hedgehog, a member of a family of putative signaling molecules, is implicated in the regulation of CNS polarity. *Cell* ***75***, 1417-1430.

Fan, L., Pepicelli, C. V., Dibble, C. C., Catbagan, W., Zarycki, J. L., Laciak, R., Gipp, J., Shaw, A., Lamm, M. L., Munoz, A. et al. (2004). Hedgehog signaling promotes prostate xenograft tumor growth. *Endocrinology* **145**, 3961-3970.

Freestone, S. H., Marker, P., Grace, O. C., Tomlinson, D. C., Cunha, G. R., Harnden, P. and Thomson, A. A. (2003). Sonic hedgehog regulates prostatic growth and epithelial differentiation. *Dev. Biol.* **264**, 352-362.

Furumoto, T. A., Miura, N., Akasaka, T., Mizutani-Koseki, Y., Sudo, H., Fukuda, K., Maekawa, M., Yuasa, S., Fu, Y., Moriya, H. et al. (1999). Notochord-dependent expression of MFH1 and PAX1 cooperates to maintain the proliferation of sclerotome cells during the vertebral column development. *Dev. Biol.* **210**, 15-29.

Gao, N., Zhang, J., Rao, M. A., Case, T. C., Mirosevich, J., Wang, Y., Jin, R., Gupta, A., Rennie, P. S. and Matusik, R. J. (2003). The role of hepatocyte nuclear factor-3 alpha (Forkhead Box A1) and androgen receptor in transcriptional regulation of prostatic genes. *Mol. Endocrinol.* **17**, 1484-1507.

Gaudet, J. and Mango, S. E. (2002). Regulation of organogenesis by the Caenorhabditis elegans FoxA protein PHA-4. *Science* **295**, 821-825.

Hayward, S. W., Baskin, L. S., Haughney, P. C., Cunha, A. R., Foster, B. A., Dahiya, R., Prins, G. S. and Cunha, G. R. (1996). Epithelial development in the rat ventral prostate, anterior prostate and seminal vesicle. *Acta Anat. (Basel)* **155**, 81-93.

Horner, M. A., Quintin, S., Domeier, M. E., Kimble, J., Labouesse, M. and Mango, S. E. (1998). pha-4, an HNF-3 homolog, specifies pharyngeal organ identity in Caenorhabditis elegans. *Genes Dev.* **12**, 1947-1952.

Hudson, D. L., Guy, A. T., Fry, P., O'Hare, M. J., Watt, F. M. and Masters, J. R. (2001). Epithelial cell differentiation pathways in the human prostate: identification of intermediate phenotypes by keratin expression. *J. Histochem. Cytochem.* **49**, 271-278.

Hynes, M., Stone, D. M., Dowd, M., Pitts-Meek, S., Goddard, A., Gurney, A. and Rosenthal, A. (1997). Control of cell pattern in the neural tube by the zinc finger transcription factor and oncogene Gli-1. *Neuron* **19**, 15-26.

Ingham, P. W. and McMahon, A. P. (2001). Hedgehog signaling in animal development: paradigms and principles. *Genes Dev.* **15**, 3059-3087.

Jaskoll, T., Leo, T., Witcher, D., Ormestad, M., Astorga, J., Bringas, P., Jr, Carlsson, P. and Melnick, M. (2004). Sonic hedgehog signaling plays an essential role during embryonic salivary gland epithelial branching morphogenesis. *Dev. Dyn.* **229**, 722-732.

Kalb, J. M., Lau, K. K., Goszczynski, B., Fukushige, T., Moons, D., Okkema, P. G. and McGhee, J. D. (1998). pha-4 is Ce-fkh-1, a fork head/HNF-3alpha, beta, gamma homolog that functions in organogenesis of the C. elegans pharynx. *Development* **125**, 2171-2180.

Karhadkar, S. S., Bova, G. S., Abdallah, N., Dhara, S., Gardner, D., Maitra, A., Isaacs, J. T., Berman, D. M. and Beachy, P. A. (2004). Hedgehog signalling in prostate regeneration, neoplasia and metastasis. *Nature* **431**, 707-712.

Kasper, S. and Matusik, R. J. (2000). Rat probasin: structure and function of an outlier lipocalin. *Biochim. Biophys. Acta* **1482**, 249-258.

Kim, M. J., Cardiff, R. D., Desai, N., Banach-Petrosky, W. A., Parsons, R., Shen, M. M. and Abate-Shen, C. (2002). Cooperativity of Nkx3.1 and Pten loss of function in a mouse model of prostate carcinogenesis. *Proc. Natl. Acad. Sci. USA* **99**, 2884-2889.

Kopachik, W., Hayward, S. W. and Cunha, G. R. (1998). Expression of hepatocyte nuclear factor-3alpha in rat prostate, seminal vesicle, and bladder. *Dev. Dyn.* **211**, 131-140.

Krebs, O., Schreiner, C. M., Scott, W. J., Jr, Bell, S. M., Robbins, D. J., Goetz, J. A., Alt, H., Hawes, N., Wolf, E. and Favor, J. (2003). Replicated anterior zeugopod (raz): a polydactylous mouse mutant with lowered Shh signaling in the limb bud. *Development* **130**, 6037-6047.

Kurita, T., Medina, R. T., Mills, A. A. and Cunha, G. R. (2004). Role of p63 and basal cells in the prostate. *Development* **131**, 4955-4964.

Lamm, M. L., Podlasek, C. A., Barnett, D. H., Lee, J., Clemens, J. Q., Hebner, C. M. and Bushman, W. (2001). Mesenchymal factor bone morphogenetic protein 4 restricts ductal budding and branching morphogenesis in the developing prostate. *Dev. Biol.* **232**, 301-314.

Lamm, M. L., Catbagan, W. S., Laciak, R. J., Barnett, D. H., Hebner, C. M., Gaffield, W., Walterhouse, D., Iannaccone, P. and Bushman, W. (2002). Sonic hedgehog activates mesenchymal Gli1 expression during prostate ductal bud formation. *Dev. Biol.* **249**, 349-366.

Lessard, J. L. (1988). Two monoclonal antibodies to actin: one muscle selective and one generally reactive. *Cell Motil. Cytoskeleton* **10**, 349-362.

Mahlapuu, M., Enerback, S. and Carlsson, P. (2001). Haploinsufficiency of the forkhead gene Foxf1, a target for sonic hedgehog signaling, causes lung and foregut malformations. *Development* **128**, 2397-2406.

Marker, P. C., Donjacour, A. A., Dahiya, R. and Cunha, G. R. (2003). Hormonal, cellular, and molecular control of prostatic development. *Dev. Biol.* **253**, 165-174.

Mirosevich, J., Gao, N. and Matusik, R. J. (2005). Expression of Foxa transcription factors in the developing and adult murine prostate. *Prostate* **62**, 339-352.

Niemann, C., Unden, A. B., Lyle, S., Zouboulis, C., Toftgard, R. and Watt, F. M. (2003). Indian hedgehog and beta-catenin signaling: role in the sebaceous lineage of normal and neoplastic mammalian epidermis. *Proc. Natl. Acad. Sci. USA* **100**, 11873-11880.

Peterson, R. S., Clevidence, D. E., Ye, H. and Costa, R. H. (1997). Hepatocyte nuclear factor-3 alpha promoter regulation involves recognition by cell-specific factors, thyroid transcription factor-1, and autoactivation. *Cell Growth Differ.* **8**, 69-82.

Podlasek, C. A., Barnett, D. H., Clemens, J. Q., Bak, P. M. and Bushman, W. (1999). Prostate development requires Sonic hedgehog expressed by the urogenital sinus epithelium. *Dev. Biol.* **209**, 28-39.

Pu, Y., Huang, L. and Prins, G. S. (2004). Sonic hedgehog-patched Gli signaling in the developing rat prostate gland: lobe-specific suppression by neonatal estrogens reduces ductal growth and branching. *Dev. Biol.* **273**, 257-275.

Qian, J., Kumar, A., Szucsik, J. C. and Lessard, J. L. (1996). Tissue and developmental specific expression of murine smooth muscle gamma-actin fusion genes in transgenic mice. *Dev. Dyn.* **207**, 135-144.

Sahlen, G. E., Egevad, L., Ahlander, A., Norlen, B. J., Ronquist, G. and Nilsson, B. O. (2002). Ultrastructure of the secretion of prostasomes from benign and malignant epithelial cells in the prostate. *Prostate* **53**, 192-199.

Sanchez, P., Hernandez, A. M., Stecca, B., Kahler, A. J., DeGueme, A. M., Barrett, A., Beyna, M., Datta, M. W., Datta, S. and Altaba, A. (2004). Inhibition of prostate cancer proliferation by interference with SONIC

HEDGEHOG-GLI1 signaling. *Proc. Natl. Acad. Sci. USA* **101**, 12561-12566.

Sasaki, H., Hui, C., Nakafuku, M. and Kondoh, H. (1997). A binding site for Gli proteins is essential for HNF-3beta floor plate enhancer activity in transgenics and can respond to Shh in vitro. *Development* **124**, 1313-1322.

Schneider, A., Brand, T., Zweigerdt, R. and Arnold, H. (2000). Targeted disruption of the Nkx3.1 gene in mice results in morphogenetic defects of minor salivary glands: parallels to glandular duct morphogenesis in prostate. *Mech. Dev.* **95**, 163-174.

Shih, D. Q., Navas, M. A., Kuwajima, S., Duncan, S. A. and Stoffel, M. (1999). Impaired glucose homeostasis and neonatal mortality in hepatocyte nuclear factor 3alpha-deficient mice. *Proc. Natl. Acad. Sci. USA* **96**, 10152-10157.

Sheng, T., Li, C., Zhang, X., Chi, S., He, N., Chen, K., McCormick, F., Gatalica, Z. and Xie, J. (2004). Activation of the hedgehog pathway in advanced prostate cancer. *Mol. Cancer* **3**, 29.

Shou, J., Ross, S., Koeppen, H., De Sauvage, F. J. and Gao, W. Q. (2001). Dynamics of notch expression during murine prostate development and tumorigenesis. *Cancer Res.* **61**, 7291-7297.

Signoretti, S., Waltregny, D., Dilks, J., Isaac, B., Lin, D., Garraway, L., Yang, A., Montironi, R., McKeon, F. and Loda, M. (2000). p63 is a prostate basal cell marker and is required for prostate development. *Am. J. Pathol.* **157**, 1769-1775.

Sinner, D., Rankin, S., Lee, M. and Zorn, A. M. (2004). Sox17 and beta-catenin cooperate to regulate the transcription of endodermal genes. *Development* **131**, 3069-3080.

Tanaka, M., Komuro, I., Inagaki, H., Jenkins, N. A., Copeland, N. G. and Izumo, S. (2000). Nkx3.1, a murine homolog of Ddrosophila bagpipe, regulates epithelial ductal branching and proliferation of the prostate and palatine glands. *Dev. Dyn.* **219**, 248-260.

Thayer, S. P., di Magliano, M. P., Heiser, P. W., Nielsen, C. M., Roberts, D. J., Lauwers, G. Y., Qi, Y. P., Gysin, S., Fernandez-del Castillo, C., Yajnik, V. et al. (2003). Hedgehog is an early and late mediator of pancreatic cancer tumorigenesis. *Nature* **425**, 851-856.

Thibert, C., Teillet, M. A., Lapointe, F., Mazelin, L., Le Douarin, N. M. and Mehlen, P. (2003). Inhibition of neuroepithelial patched-induced apoptosis by sonic hedgehog. *Science* **301**, 843-846.

Thomson, A. A. and Cunha, G. R. (1999). Prostatic growth and development are regulated by FGF10. *Development* **126**, 3693-3701.

Thomson, A. A., Foster, B. A. and Cunha, G. R. (1997). Analysis of growth factor and receptor mRNA levels during development of the rat seminal vesicle and prostate. *Development* **124**, 2431-2439.

Wan, H., Dingle, S., Xu, Y., Besnard, V., Kaestner, K. H., Ang, S. L., Wert, S., Stahlman, M. T. and Whitsett, J. A. (2005). Compensatory roles of Foxa1 and Foxa2 during lung morphogenesis. *J. Biol. Chem.* **14**, 13809-13816.

Wang, B. E., Shou, J., Ross, S., Koeppen, H., De Sauvage, F. J. and Gao, W. Q. (2003). Inhibition of epithelial ductal branching in the prostate by sonic hedgehog is indirectly mediated by stromal cells. *J. Biol. Chem.* **278**, 18506-18513.

Wang, X. D., Shou, J., Wong, P., French, D. M. and Gao, W. Q. (2004). Notch1-expressing cells are indispensable for prostatic branching morphogenesis during development and re-growth following castration and androgen replacement. *J. Biol. Chem.* **279**, 24733-24744.

Wang, Y., Hayward, S. W., Donjacour, A. A., Young, P., Jacks, T., Sage, J., Dahiya, R., Cardiff, R. D., Day, M. L. and Cunha, G. R. (2000). Sex hormone-induced carcinogenesis in Rb-deficient prostate tissue. *Cancer Res.* **60**, 6008-6017.

Wang, Y., Hayward, S., Cao, M., Thayer, K. and Cunha, G. (2001). Cell differentiation lineage in the prostate. *Differentiation* **68**, 270-279.

Weaver, M., Batts, L. and Hogan, B. L. (2003). Tissue interactions pattern the mesenchyme of the embryonic mouse lung. *Dev. Biol.* **258**, 169-184.

Weigel, D. and Jackle, H. (1990). The fork head domain: a novel DNA binding motif of eukaryotic transcription factors? *Cell* **63**, 455-456.

Wells, J. M. and Melton, D. A. (1999). Vertebrate endoderm development. *Annu. Rev. Cell Dev. Biol.* **15**, 393-410.

Yamagishi, H., Maeda, J., Hu, T., McAnally, J., Conway, S. J., Kume, T., Meyers, E. N., Yamagishi, C. and Srivastava, D. (2003). Tbx1 is regulated by tissue-specific forkhead proteins through a common Sonic hedgehog-responsive enhancer. *Genes Dev.* **17**, 269-281.

Yu, J., Carroll, T. J. and McMahon, A. P. (2002). Sonic hedgehog regulates proliferation and differentiation of mesenchymal cells in the mouse metanephric kidney. *Development* **129**, 5301-5312.

Zaret, K. (1999). Developmental competence of the gut endoderm: genetic potentiation by GATA and HNF3/fork head proteins. *Dev. Biol.* **209**, 1-10.

Zaret, K. S. (2002). Regulatory phases of early liver development: paradigms of organogenesis. *Nat. Rev. Genet.* **3**, 499-512.